Sciencexpress Report

Strong Release of Methane on Mars in Northern Summer 2003

Michael J. Mumma,[1]* Geronimo L. Villanueva,[2,3] Robert E. Novak,[4] Tilak Hewagama,[3,5] Boncho P. Bonev,[2,3] Michael A. DiSanti,[3] Avi M. Mandell,[3] Michael D. Smith[3]

[1]NASA Goddard Space Flight Center, Mailstop 690.3, Greenbelt, MD 20771, USA. [2]Department of Physics, Catholic University of America, Washington, DC 20008, USA. [3]NASA Goddard Space Flight Center, Mailstop 693, Greenbelt, MD 20771, USA. [4]Department of Physics, Iona College, New Rochelle, NY 10801, USA. [5]Department of Astronomy, University of Maryland, College Park, MD 20742-2421, USA.

*To whom correspondence should be addressed. E-mail: michael.j.mumma@nasa.gov

Living systems produce more than 90% of Earth's atmospheric methane; the balance is of geochemical origin. On Mars, methane could be a signature of either origin. Using high-dispersion infrared spectrometers at three ground-based telescopes, we measured methane and water vapor simultaneously on Mars over several longitude intervals in (northern) early- and late-summer 2003 and near vernal equinox 2006. When present, methane occurred in extended plumes and the maxima of latitudinal profiles imply that the methane was released from discrete regions. At northern mid-summer, the principal plume contained ~19,000 metric tons of methane and the estimated source strength (≥ 0.6 kg s^{-1}) was comparable to that of the massive hydrocarbon seep at Coal Oil Point (Santa Barbara, CA).

The atmosphere of Mars is strongly oxidized, composed primarily of carbon dioxide (CO_2, 95.3%) along with minor nitrogen (N_2, 2.7%), carbon monoxide (CO, 0.07%), oxygen (O_2, 0.13%), water vapor (H_2O, 0–300 ppm), and radiogenic argon (1.6%); other species and reduced gases such as methane (CH_4) are rare. CH_4 production by atmospheric chemistry is negligible and its lifetime against removal by photochemistry is estimated to be several hundred years (*1–3*) or shorter if strong oxidants such as peroxides are present in the surface or on airborne dust grains (*4*). Thus, the presence of significant methane would require recent release from sub-surface reservoirs; the ultimate origin of this methane is uncertain, but it could be either abiotic or biotic (*2, 5, 6*).

Before 2003, all searches for methane were negative (*7–9*). Since then, three groups have reported detections of methane (*10–14*); see (*15–20*) for discussion. Spectral data from Mars Express contain five unidentified spectral features between 3000 and 3030 cm^{-1}, of which one coincides with the expected position of the CH_4 Q-branch (*11, 14 ,21*). The data span all seasons and extend over several years, but low S/N ratios require averaging the spectra over two of the three key dimensions (longitude, latitude, time). Other searches featured low spatial (*12*) or sparse seasonal coverage (*12, 13*), and the results (methane mixing ratios) are best interpreted as upper limits.

We report measurements of methane in Northern Summer 2003 and estimate its source strength and its (short) destruction lifetime. Our search covered about 90% of the planet's surface and spanned 3 Mars years (7 Earth years). Our results (*10*) are based on simultaneous detection of multiple spectrally-resolved lines of methane, and each observation is spatially resolved, allowing examination of spatial and temporal effects. Our spatial maps reveal local sources and seasonal variations.

To search for methane and other gases on Mars, we used the high-dispersion infrared spectrometers at three ground-based telescopes. Here we report data from CSHELL/IRTF (Hawaii) and NIRSPEC/Keck-2 (Hawaii) (SOM-1). Each spectrometer features a long entrance slit that is held to the central meridian of Mars (Fig. 1A) while spectra are taken sequentially in time (e.g., fig. S1). Pixelated spectra were acquired simultaneously at contiguous positions along the entire slit length, for each observation, providing 35 spectra at 0.2 arc-second (arc-sec) intervals (~195 km at disk center) when Mars' diameter is 7 arc-sec (e.g., Fig. 1A). We binned these data (e.g., in groups of 3 along the slit) to provide latitudinally resolved spectra, and then in time (longitude) to improve the S/N ratio (SOM-1). Here, we focus on three dates in 2003 (UT Jan. 12, UT March 19 & 20) and on UT Feb. 26, 2006 (Table 1).

Our spectra exhibit strong lines of terrestrial H_2O ($2\nu_2$ band) and CH_4 (ν_3) along with weaker lines of O_3 ($3\nu_3$) seen against the continuum (Fig. 1, B and C, top). We corrected the data for telluric extinction (SOM-2). At 3.3 μm, Mars is seen mainly in reflected sunlight, so the collected spectra also contain Fraunhofer lines (SOM-3). Removing these two components from a composite spectrum exposed the residual Mars atmospheric spectrum (Fig. 1, B and C) (*22*). One line of CH_4 and three distinct lines of H_2O are seen in each panel.

Methane consists of three separate nuclear spin species (A, E, F) that act as independent spectral entities. The

identification of two spectrally resolved methane lines (R0 and R1, of the A and F species, respectively) and the good agreement (within measurement error) of the CH_4 column densities obtained independently from each line support our detection (systematic uncertainty and stochastic errors are discussed in SOM-2 and SOM-3). At a later season (L_s = 220°), we detected the P2 doublet consisting of lines of the E and F species (SOM-1, fig. S2). Detections (or upper limits) reported by others are based on the intensity summed over the frequencies of multiple unresolved lines [the Q-branch (*11*, *14*)] or on the summed intensity of several undetected individual lines (*12*, *13*).

Column densities and mixing ratios for methane obtained from the spectra of Fig. 1 show a broad methane plume in late-summer when averaged over 46° longitude (Fig. 2, A and B) (SOM-3); using more restricted longitudinal binning shows higher maxima (Fig. 2C, profile d). In early spring (profile a), the CH_4 mixing ratio was small at all latitudes, and showed only a hint of the marked maximum seen in late summer. By early summer (profiles b and c), methane was prominent but the maximum mixing ratio occurred at more northerly latitudes and was somewhat smaller than in late summer. The late summer profile (d) in Fig. 2C differs from the profile shown in Fig. 2B, owing to different longitudinal binning (*23*). The mixing ratios shown in Fig. 2C (profile d) represent a subset of the data of Fig. 1B, centered at CML 310° (see aspect, Fig. 1A) and binned over only 30 minutes. Including the slit width, 30-minute binning provides a footprint at the sub-Earth point that spans ~16° (948 km) in longitude and 10° (586 km) in latitude (fig. S1, Table 1).

A quantitative release rate can be inferred by considering the observed temporal changes (with season) and measured spatial profiles. The summer mixing ratios (profiles b, c, d) show a clear maximum for each north-south spatial profile (Fig. 2C). Moving southward by about 30° from the latitude of the peak, the mixing ratio decreased by a factor of two in each case, and for profile d the northward gradient was similar to the southward one. These latitudinal gradients suggest that there was a local source(s) and the resulting plume(s) was being dispersed by atmospheric circulation.

We consider the dimension of the hypothesized methane plume to be about 60° in latitude (full width at half maximum, Fig. 2C, profile d), and assume a similar dimension in longitude. The latter view is weakly supported by profiles b and c, which differ by 27° in central longitude and by a factor of two in peak mixing ratio. It is also supported by the profile formed by binning over 46° in longitude (277°-323°, Fig. 2B) which has a peak mixing ratio (24 ppb) reduced by a factor of two from the peak value (45 ppb) obtained when binning over only 16° of longitude (302°-318°, Fig. 2C, profile d). The slight increase of profile d near 40° N is consistent with enhanced methane (perhaps owing to continued release at that latitude - compare profiles b and c), while the slight increase in profile c near 15° S suggests a small contribution from a source to the west (compare peak position, profile d). Together, these profiles suggest that there may be two local source regions, the first centered near (30° N, 260° W) and the second near (0°, 310° W). The vapor plume from each is consistent with ~ 60° in both latitude and longitude.

The amount of trace gas present in each plume can be estimated from these parameters (SOM-4). In the central plume of profile d (FWHM diameter ~ 60°), the mean CH_4 mixing ratio is ~ 33 ppb (120 mol km^{-2}), and the plume contains ~ 1.17 x 10^9 moles of CH_4 (~1.86 x 10^7 kg, or ~19,000 metric tons). If seasonally controlled, the duration of release must be substantially shorter than 0.5 Mars years, requiring a mean CH_4 release rate ≥ 39 mol s^{-1} (≥ 0.63 kg s^{-1}). For comparison, the massive hydrocarbon seep field at Coal Oil Point (Santa Barbara, CA) releases methane at a rate of ~0.4 - 1.0 kg s^{-1} (*24*).

We considered three models for plume formation, to constrain aspects of methane release and its migration in latitude and longitude (SOM-5). A model based on release from a central source region coupled with eddy diffusion fits the observed plume parameters. Models of meridional flow using a GCM (Global Circulation Model) suggest that released gas would move northward by ~3.3 cm s^{-1} at this season (*25*), for a total displacement by not more than ~170 km from its central source. If the mixing coefficients (K_x, K_y) in zonal and meridional directions are identical (K_h), a steady source would fill the plume (profile d) in 60 days if K_h ~ 6.4 x 10^8 cm^2 s^{-1}. For this case, the required source strength was ~ 3.66 kg s^{-1}. The filling time and K_h vary inversely, whereas K_h and source strength vary proportionately. For a filling time of 0.5 Mars yr (~344 Earth days), K_h ~ 1.1 x 10^8 cm^2 s^{-1} and the source strength was ~0.63 kg s^{-1}. A reasonable limit for filling time (< 120 days) requires K_h ~3.2 x 10^8 cm^2 s^{-1} and source strength ~ 1.8 kg s^{-1}.

These parameters are consistent with release from a single central source region, followed by efficient eddy mixing (SOM-5). The central source could be activated thermally by warming of a surface zone, or by connecting sub-permafrost regions to the atmosphere through seasonally opened pores in scarps or crater walls. The plume would reflect the gross morphology of active release zones (and their intensity), and the peak could suggest a region of enhanced release. For comparison, the sub-Solar latitude was 24º N at L_s =122º (compare profiles b and c) and 10º N for L_s = 155º (profile d).

Additional information is obtained from a high-resolution map constructed from our data for mid-summer 2003 (Fig. 3 and fig. S1). Methane appears notably enriched over several localized areas: A (East of Arabia Terra, where we also measure greatly enriched water vapor), B1 (Nili Fossae), and

B2 (SE quadrant of Syrtis Major). Unusual enrichments of hydrated minerals (phyllosilicates) were identified in Nili Fossae from Mars Express (*26*, *27*) and from the Mars Reconnaissance Orbiter (*28*) (Fig. 3). The observed morphology and mineralogy (*29*, *30*) of this region suggest that these bedrock outcrops, rich in hydrated minerals, might be connecting with reservoirs of buried material rich in volatile species. The characteristic arcuate ridges in the southeast quadrant of Syrtis Major were interpreted as consistent with catastrophic collapse of that quadrant, from interaction with a volatile-rich substrate (*30*).

The low mean abundance measured in early spring 2006 (profile a) provides an important constraint on the methane lifetime. The plume seen in March 2003 (19,000 tons, Fig. 2C, profile d) implies a global mean mixing ratio of ~2 ppb, if later spread uniformly over the planet. The content of the central plume of profile c is similar. Combining data for the entire region mapped during northern summer brings the total methane to 42,000 tons, or 6 ppb if spread uniformly over the planet. However, the mean mixing ratio displayed in early spring equinox in 2006 (profile a, Fig. 2C) was only 3 ppb (SOM-3). If methane is not removed by other means, the implied destruction lifetime is ~ 4 Earth years if the 2003 event was singular, to as little as ~0.6 Earth years if the event repeats each Mars year. In either case, the destruction lifetime for methane is much shorter than the timescale (~350 years) estimated for photochemical destruction [e.g., (*12*)]. Another process thus must dominate removal of atmospheric methane on Mars and it must be more efficient than photochemistry by a factor ≥100.

Heterogeneous (gas-grain) chemistry is a strong candidate. The presence of strong oxidants in the soil was suggested first by the labeled-release experiment on Viking landers, and laboratory simulations suggested that peroxides (e.g., H_2O_2) were responsible; the apparent discovery of perchlorate ($XClO_4$) by the Phoenix lander (*31*, *32*) suggests the existence of another family of strong oxidants, although their presence at low latitudes has not been established. Lofting oxidant-coated soil particles into the atmosphere could permit rapid oxidation of CH_4 that collides with them. H_2O_2 is also produced photochemically and is a known trace gas in the atmosphere (*33*), and (being polar) might bind to aerosol surfaces. Electrochemical processes in dust storms may produce additional peroxide efficiently (*4*, *6*, *19*, *20*) (SOM-6). Peroxide coated grains might provide an efficient sink for methane for many years thereafter if they settle to the surface and are sequestered in the regolith (*6*, *20*). Sequestered oxidants should also efficiently destroy upward-diffusing methane, reducing the fraction that might escape to the atmosphere.

The most compelling question relates to the origin of methane on Mars. The methane we detected is of unknown age – its origin could be ancient (*34*) or perhaps recent. Both geochemical and biological origins have been explored, but no consensus has emerged. Most theses draw upon known terrestrial analogues such as production in magma (*15*, *16*) or serpentinization of basalt [e.g., (*35*)]), or production by psychrophilic methanogenic biota in Mars-analogue cryo-regimes such as permafrost (*17*). The annual release of methane from an arctic tundra landscape (at 72° N) was measured to be 3.15 g m^{-2}, with mid-summer CH_4 fluxes of typically 30 mg m^{-2} day^{-1} (*36*). If similar release rates applied to our mid-summer plume, the tundra-equivalent-area of (assumed uniform) release would be ~ 6000 km^2 compared with a plume footprint ~ 9.7 x10^6 km^2. If methane release were uniform over the plume footprint, the mean release rate could be smaller than the arctic rate by a factor of ~1600.

Of special interest are the deep bio-communities that utilize H_2 (produced by radiolysis of water) as an energy source (reducing CO_2 to CH_4). These communities thrive at 2-3 km depth in the Witwatersrand Basin of South Africa and have been isolated from the surface (and photosynthesis) for millions of years (*37*, *38*). It might be possible for analogous biota to survive for eons below the cryosphere boundary on Mars, where water is again liquid, radiolysis can supply energy, and CO_2 can provide carbon. Gases accumulated in such zones might be released to the atmosphere if pores or fissures open seasonally, connecting these deep zones to the atmosphere at scarps, crater walls, or canyons. The location of methane maxima over the Syrtis Major shield volcano and the nearby Nili Fossae district suggests a possible relation to serpentinization and/or to the phyllosilicates discovered there (*39*, *40*).

References and Notes

1. H. Nair, M. Allen, A. D. Anbar, Y. L. Yung, R. T. Clancy, *Icarus* **111**, 124 (1994).
2. M. E. Summers, B. J. Lieb, E. Chapman, Y. L. Yung, *Geophys. Res. Lett.* **29**, 2171 (2002).
3. Ah-S. Wong, S. K. Atreya, T. Encrenaz, *J. Geophys. Res. (Planets)* **108**, 7-1 (2003).
4. S. K. Atreya *et al.*, *Astrobiology* **6**, 439 (2006).
5. R. E. Pellenbarg, M. D. Max, S. M. Clifford, *J. Geophys. Res. (Planets)* **108**, GDS 23-1 (2003).
6. S. K. Atreya, P. R. Mahaffy, and Ah-S. Wong, *Planet. Sp. Sci.* **55**, 358 (2007).
7. W. C. Maguire, *Icarus* **32**, 85 (1977).
8. V. A. Krasnopolsky, G. L. Bjoraker, M. J. Mumma, D. E. Jennings, *J. Geophys. Res.* **102**, 6525 (1997).
9. M. Lellouch *et al.*, *Planet. Sp. Sci.* **48**, 1393 (2000).
10. M. J. Mumma *et al.*, *Bull. Am. Astron. Soc.* **35**, 937 (2003); **36**, 1127 (2004); **37**, 669 (2005); **39**, 471 (2007); **40**, 396 (2008).
11. V. Formisano, S. Atreya, T. Encrenaz, N. Ignatiev, M. Giuranna, *Science* **306**, 1758 (2004).

12. V. A. Krasnopolsky, J. P. Maillard, T. C. Owen, *Icarus* **172**, 537 (2004).
13. V. A. Krasnopolsky, *Icarus* **190**, 93 (2007).
14. A. Geminale, V. Formisano, M. Giuranna, *Planet. Sp. Sci.* **56**, 1194 (2008).
15. J. R. Lyons, C. E. Manning, C. E. Nimmo, *Geophys. Res. Lett.* **32**, L13201(2005).
16. C. Oze and M. Sharma, *Geophys. Res. Lett*. **32**, L10203 (2005).
17. T. C. Onstott *et al.*, *Astrobiology* **6**, 377 (2006).
18. V. A. Krasnopolsky, *Icarus* **180**, 359 (2006).
19. W. M. Farrell, G. T. Delory, S. K. Atreya, *Geophys. Res. Lett.* **33**, L21203 (2006).
20. G. T. Delory *et al.*, *Astrobiology* **6**, 451 (2006).
21. V. Formisano *et al.*, *Planet. Sp. Sci.* **53**, 1043 (2005).
22. G. L. Villanueva, M. J. Mumma, R. E. Novak, T. Hewagama, *Icarus* **195**, 34 (2008).
23. We binned spectra over 46° degrees of longitude (centered at CML 300°) for Fig. 1, B and C (and Fig. 2, A and B), but over only 16° for Fig. 2C. Profile d is centered at CML 310°, leading to lower mean mixing ratios in Fig. 2B compared with Fig. 2C (profile d). See detailed map in Fig. 3.
24. S. Mau *et al.*, *Geophys. Res. Lett.* **34**, L22603 (2007).
25. M. A. Mischna, M. I. Richardson, R. J. Wilson, D. J. McCleese, *J. Geophys. Res*. **108**, 5062, 16-1 (2003).
26. F. Poulet et al., *Nature* **438**, 623 (2005).
27. J. P. Bibring et al., *Science* **312**, 400 (2006).
28. J. F. Mustard et al., *Nature* **454**, 305 (2008).
29. H. Hiesinger and J. W. Head III, *J. Geophys. Res*. **109**, E01004 (2004).
30. D. Baratoux et al., *J. Geophys. Res*. **112**, E08S05 (2007).
31. M. H. Hecht *et al.*, *Eos* **89**, Fall Meeting Suppl., Abstr. U14A-04 (2008).
32. S. P. Kounaves *et al.*, *Eos* **89**, Fall Meeting Suppl., Abstr. U14A-05 (2008).
33. T. Encrenaz *et al.*, *Icarus* **195**, 547 (2008).
34. M. D. Max, S. M. Clifford, *J. Geophys. Res.* **105**, 4165 (2000).
35. D. S. Kelley *et al.*, *Science* **307**, 1428 (2005).
36. C. Wille, L. Kutzbach, T. Sachs, D. Wagner, E.-M. Pfeiffer, *Global Change Biol.* **14**, 1395 (2008).
37. T. C. Onstott *et al.*, *Geomicrobiol. J.* **23**, 369 (2006).
38. B. Sherwood Lollar *et al.*, *Chem. Geol.* **226**, 328 (2006).
39. J.-P. Bibring *et al.*, *Science* **312**, 400 (2006).
40. J. F. Mustard *et al.*, *Nature* **454** (7202), 305 (2008).
41. R. Greeley, J. E. Guest, U.S. Geol. Surv, Map I-1802-B (1987).
42. D. E. Smith *et al.*, *J. Geophys. Res*. **106**, 23689 (2001).
43. We thank T. C. Onstott for helpful comments, and two anonymous referees for their comments and suggestions. This work was supported by NASA [Planetary Astronomy Program (RTOP 344-32-07 to M.J.M), Astrobiology Institute (RTOP 344-53-51, to M.J.M), and Postdoctoral Program (G.L.V.)] and by NSF (Research at Undergraduate Institutions Program AST-0505765, to R.E.N.). We thank the Director and staff of NASA's InfraRed Telescope Facility (operated for NASA by the University of Hawaii) for exceptional support throughout our long Mars observing Program. Data were also obtained at the W. M. Keck Observatory, operated as a scientific partnership by CalTech, UCLA, and NASA.

Supporting Online Material

www.sciencemag.org/cgi/content/full/1165243/DC1
SOM Text
Figs. S1 to S6
References and Notes

28 August 2008; accepted 6 January 2009
Published online 15 January 2009; 10.1126/science/1165243
Include this information when citing this paper.

Fig. 1. Detections of methane and water vapor on Mars on UT 19 and 20 March 2003. (**A**) Mars is shown as it appeared at the mean time of the R0 and R1 observations (Table 1). The sub-Solar (*) and sub-Earth (+) points are marked, along with several prominent features. Contours of constant altitude are shown at intervals of 3 km, and regions beyond the afternoon terminator (night-side) appear in grey. The entrance slit of the spectrometer was oriented N-S on Mars along the central meridian, and is shown to scale. (**B**) Spectra taken on 20 March were extracted at eleven equal intervals (0.6" each) along the slit (ranging from 70° N to 70° S), after binning over longitudes 277° - 323° West. At the sub-Earth position, the binned spectrum samples a footprint 3215 km (E-W) by 586 km (N-S) (see text and SOM-1). Strong lines of terrestrial water and methane (labeled) and weak lines of ozone (e.g., 3036 - 3038 cm^{-1}) appear in a typical spectrum, shown at top of this panel. See (SOM-3) for data reduction. Narrow spectral lines of H_2O (3 lines, small dashes) and CH_4 (the R1 line, long dashes) are seen at the Doppler-shifted positions expected for this date. Corresponding Mars ozone (O_3) absorptions for this date are weak and would appear in the southern polar region (not sampled). (**C**) Spectra taken on 19 March are shown as in (B), but binned over the longitude range 289° - 335°. Spectral lines of H_2O (3 lines, small dashes) and CH_4 (the R0 line, long dashes) are seen. The longitude range sampled was systematically Westward (by 12°) of that sampled for R1 (Table 1), owing to the slower rotation of Mars relative to Earth. The residual spectra shown in (B) and (C) are scaled by a factor of either 10 or 25 (grey background), to make the lines more apparent. (**D** and **E**) show residual intensities in a grey-scale format, to visualize more easily the spatial distribution of the gases with latitude.

The lines are displayed as measured, i.e., corrections for two-way air mass on Mars (Sun to Mars-surface and Mars-surface to Earth), for Mars local topography, and for terrestrial transmittance have not yet been applied to the residuals (see Fig. 2).

Fig. 2. Absolute abundances, spatial profiles, and seasonal changes of methane on Mars. (**A**) We show the total CH_4 column density (molecules m^{-2}) along a two-way path (Sun to Mars-surface and Mars-surface to Earth) needed to reproduce the measured lines (after correcting for terrestrial transmittance, SOM-2). The R0 (Fig. 1C) and R1 (Fig. 1B) lines were analyzed independently for a range of longitudes that spanned 46° but differed by 12° in mean longitude (312° for R0 vs. 300° for R1, Table 1). The apparent differences in methane column density seen at low-latitudes (30N to 15S) reflect (in part) differences in mean topography sampled on the two dates. The confidence limits contain both systematic uncertainty and random error; the systematic uncertainty affects all extracted values in the same way while the random error introduces scatter among the individual points (SOM-2, SOM-3). (**B**) We show the local mixing ratio (ppb) of CH_4 obtained from the column density (A) in each footprint, after correcting for two-way air mass on Mars and for topography (SOM-3). The mixing ratios derived from R0 and R1 of CH_4 agree, within confidence limits. The remaining systematic difference at low-latitudes is consistent with stronger weighting of local sources (Fig. 3) on 20 March (R1) when the longitude range sampled was more nearly centered over them. The differences in mixing ratio (R0 vs. R1) should then have decreased with increasing distance from the source(s), as they did (compare values at 60N, 40N, and 25S, 35S, 47S, and 62S). (**C**) Geographic and temporal variability of Mars methane. We show latitudinal profiles of methane mixing ratios for different longitudes and seasons; the width of the color envelope represents the ± 1-σ confidence envelope. The areocentric seasons (L_S) are: early Northern Spring (a: 17º), early Northern Summer (b, c: 122º), late Northern Summer (d: 155º) (Table 1). These extracts are taken from spectra centered at the indicated longitude (CML), and the sub-Earth footprints span longitude-latitude ranges (Table 1) with these physical dimensions: a: 770 km x 535 km, b, c: 1274 km x 818 km, d: 948 km x 586 km. The mixing ratios shown in profile d are larger than those shown in Fig. 2B owing to different longitudinal binning, and they reflect the longitudinal maximum of the plume (SOM-1, fig. S1, fig. S6, and Fig. 3).

Fig. 3. Regions where methane appears notably localized in Northern Summer (A, B1, B2), and their relationship to mineralogical and geo-morphological domains. (**A**) Observations of methane near the Syrtis Major volcanic district. (**B**) Geologic map of Greeley and Guest (*41*) superimposed on the topographic shaded-relief from MOLA (*42*). The most ancient terrain (Npld, Nple) is Noachian in age (~3.6 - 4.5 billion years old, when Mars was wet), and is overlain by volcanic deposits from Syrtis Major of Hesperian (Hs) age (~3.1 - 3.6 billion yrs old). See text.

Table 1. Observational searches for Mars methane on selected dates. A complete listing of all dates searched, spanning 7 years, is available from the authors.

Date and observation range (UT)	Mars season (L_s,°)	Longitude range (CML,°)	Doppler shift (km s^{-1})	CH_4 line searched	Footprint* (°long. by °lat.)
2003 – Mars year (MY) 26					
11 Jan 19:36-20:34	121.5	274 - 288	-14.7	R1	22° x 14°
12 Jan 17:20-20:18	121.9	231 – 274	-15.0	R1	22° x 14°
13 Jan 17:05-20:07	122.4	218 - 262	-15.0	R0	22° x 14°
19 Mar 15:41-18:50	154.5	289 – 335	-15.7	R0	16° x 10°
20 Mar 15:34-18:44	155.0	277 - 323	-15.6	R1	16° x 10°
2006 – Mars year (MY) 27-28					
16 Jan 04:49-07:03†	357.3	303–336	+16.1	R0, R1	
26 Feb 01:28-02:53	17.2	223–244	+17.1	R1	13° x 10°

*Centered on the sub-Earth point, binned over 30 min in time and 0.6" along the slit.
†Using NIRSPEC/Keck (SOM-3), all other listed observations used CSHELL/IRTF.

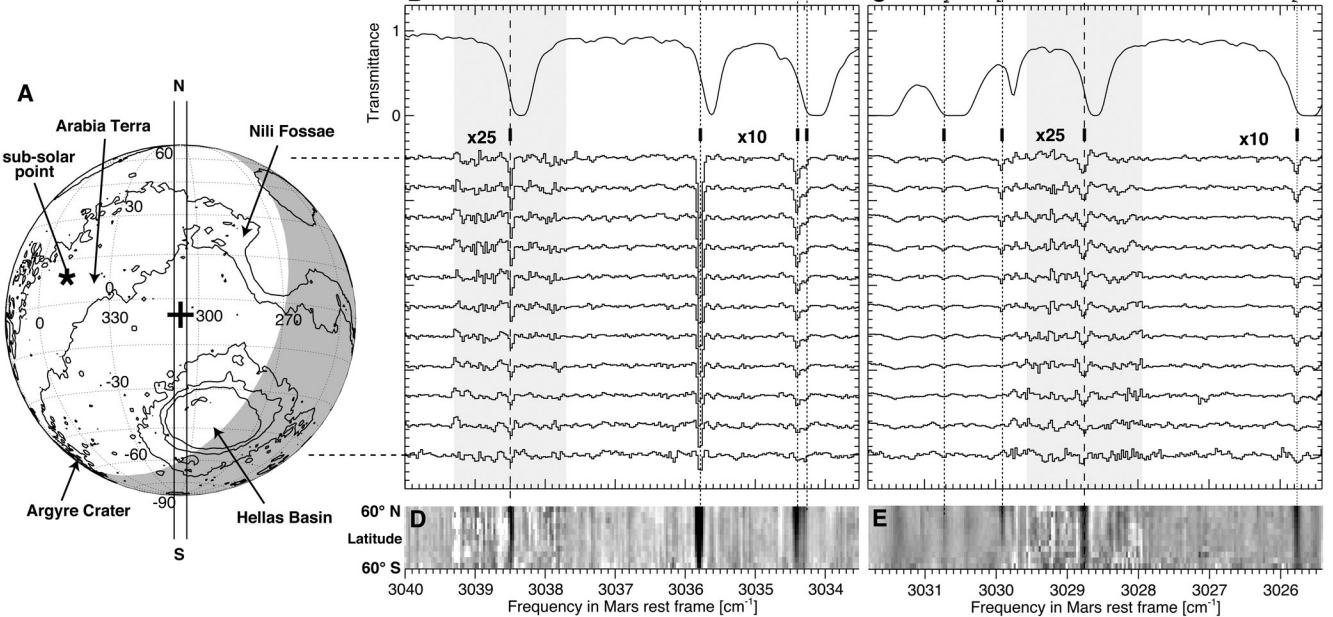
A
N
S
Arabia Terra
Nili Fossae
sub-solar point
Argyre Crater
Hellas Basin
60
30
0
-30
-60
-90
330
300
270
B
C
CH_4 - R1
H_2O
H_2O
H_2O
H_2O
CH_4 - R0
H_2O
Transmittance
1
0
x25
x10
x25
x10
D
E
60° N
Latitude
60° S
3040
3039
3038
3037
3036
3035
3034
3031
3030
3029
3028
3027
3026
Frequency in Mars rest frame [cm^{-1}]
Frequency in Mars rest frame [cm^{-1}]

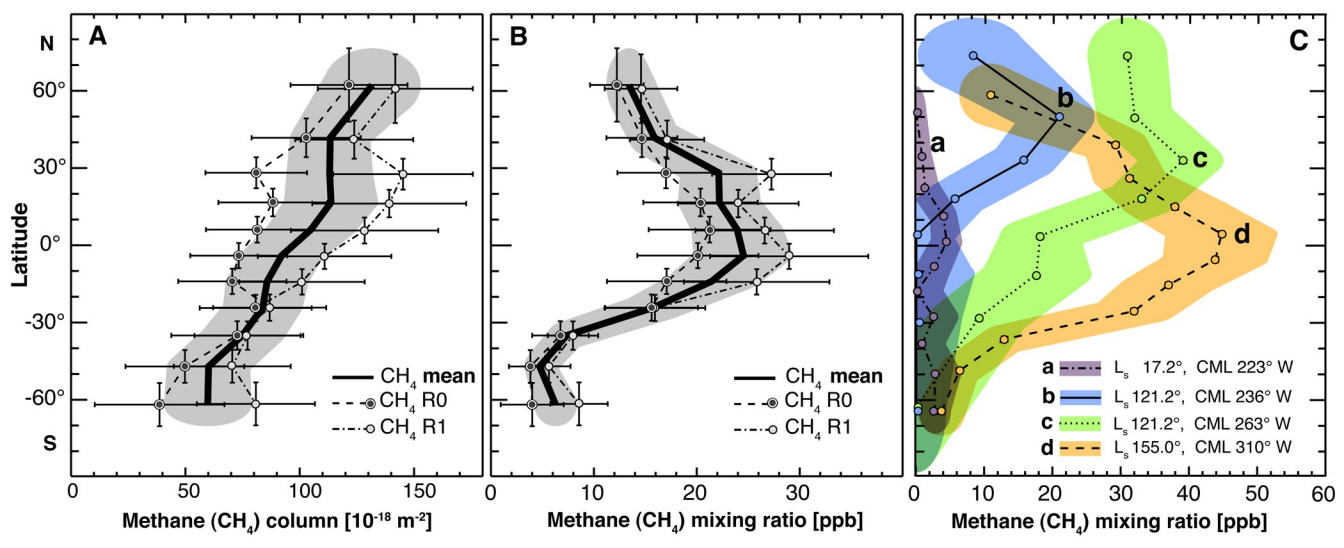
A
B
C
N
60°
30°
0°
-30°
-60°
S
Latitude
CH4 mean
CH4 R0
CH4 R1
0
50
100
150
Methane (CH4) column [10-18 m-2]
10
20
30
Methane (CH4) mixing ratio [ppb]
a
b
c
d
a Ls 17.2°, CML 223° W
b Ls 121.2°, CML 236° W
c Ls 121.2°, CML 263° W
d Ls 155.0°, CML 310° W
40
60
Methane (CH4) mixing ratio [ppb]

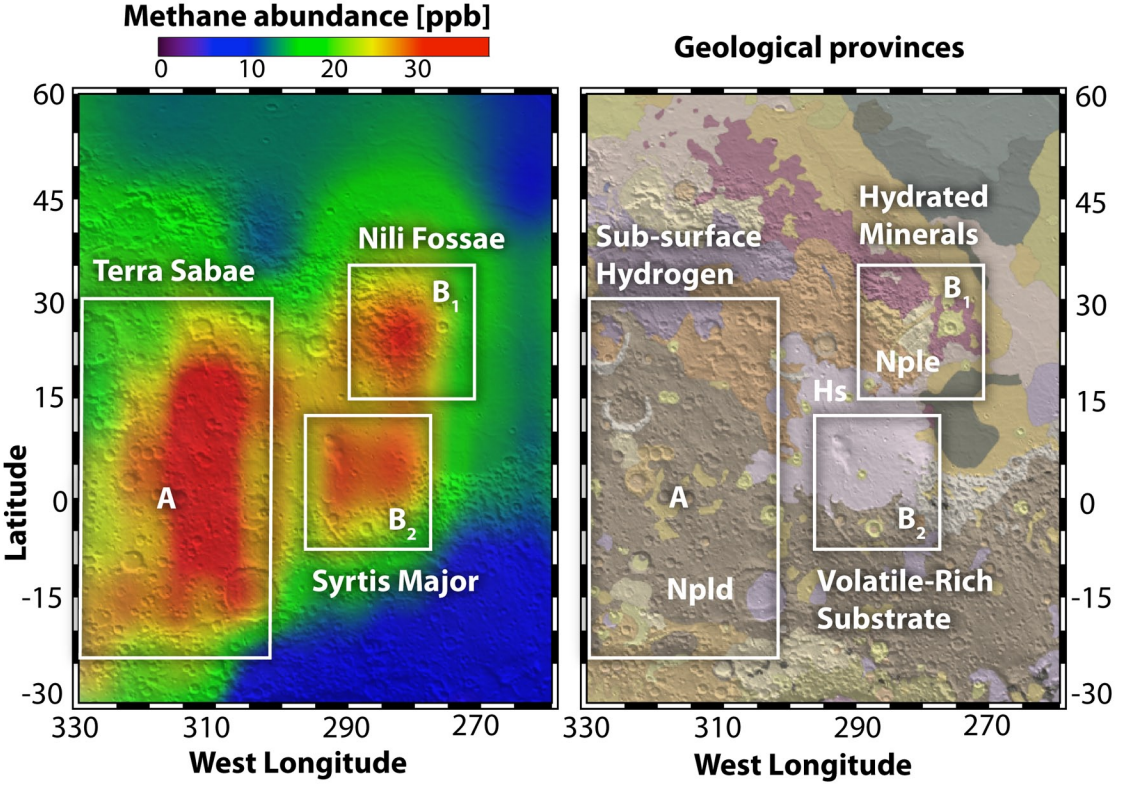
Methane abundance [ppb]
0
10
20
30
Geological provinces
Terra Sabae
Nili Fossae
B1
A
B2
Syrtis Major
Sub-surface
Hydrogen
Hydrated
Minerals
B1
Nple
Hs
A
B2
Npld
Volatile-Rich
Substrate
60
45
30
15
0
-15
-30
Latitude
330
310
290
270
West Longitude